FACTA UNIVERSITATIS
Series: **Mechanical Engineering**
https://doi.org/10.22190/FUME210102006R

Original scientific paper

MESOSCALE DEFORMATION-INDUCED SURFACE PHENOMENA IN LOADED POLYCRYSTALS

Varvara Romanova, Ruslan Balokhonov, Olga Zinovieva

Institute of Strength Physics and Materials Science, Tomsk, Russia

Abstract. *The paper reviews the results of numerical analyses for the micro-and mesoscale deformation-induced surface phenomena in three-dimensional polycrystals with the explicit account for the grain structure. The role of the free surface and grain boundaries in the appearance of the grain-scale stress concentrations and plastic strain nucleation is illustrated on the examples of aluminum polycrystals. Special attention is paid to the discussion of mesoscale deformation-induced surface roughening under uniaxial tension.*

Key words: *Polycrystals, Free surface, Grain boundaries, Deformation-induced roughness, Microstructure-based calculations, Mesomechanics*

1. INTRODUCTION

The mechanical and physical properties of material surface layers are among the key factors determining the service life of machine parts and components. This is especially evident for tribological systems where the load is directly applied to the material surface through the contact region to cause wear of the surface layers [1-4]. While it is not so evident in the absence of external forces, the free surface still plays a vital role in the deformation behavior of materials. Many surface phenomena observed in real materials take their origin from the microstructural effects and thus can hardly be described within a classical phenomenologically-based approach of continuum mechanics. For example, stresses and strains in a homogeneous specimen in the absence of geometrical nonlinearities (notches, necks, surface roughness, etc.) are distributed uniformly over the specimen sections so that cracks have even chances to nucleate near the free surface or in the bulk. However, experimental studies (e.g., [5-8]) have reported that cracks under tensile or cyclic loadings primarily nucleated on the surface or within a thin subsurface

Received January 02, 2021 / Accepted January 27, 2021
Corresponding author: Varvara Romanova
Institute of Strength Physics and Materials Science SB RAS, Akademicheskii prospect 2/4, 634055 Tomsk, Russia
E-mail: varvara@ispms.tsc.ru

© 2020 by University of Niš, Serbia | Creative Commons License: CC BY-NC-ND

layer. In order to describe this effect, we should go down from the macro to lower scales where the material is inhomogeneous.

Another prominent example of the microstructure-related surface phenomena is deformation-induced roughening, inevitably accompanying plastic deformation in polycrystalline metals and alloys. The specimen free surface becomes rough even in the conditions of uniaxial or biaxial tension where no external forces act perpendicular to the specimen surface to cause any out-of-plane surface displacements [8-11]. Again this behavior is failed to be predicted by macroscopic continuum mechanics but should be described in terms of micromechanics to take into account non-linear deformation modes attributed to the microstructural inhomogeneity.

This paper reviews the results of numerical analyses for the free surface effects on the stress-strain evolution in quasistatically loaded polycrystals where the 3D grain structure is taken into account explicitly. Special attention is given to the examination of surface phenomena at the mesoscale where individual grains are united into clusters to form rough patterns on the free surface.

2. MICROSTRUCTURE-BASED SIMULATION

Let us briefly discuss the computational approach in use while its detailed description is given elsewhere (see, e.g., [12-14]). The numerical simulation involves the finite-difference [12] or finite-element solutions [13-15] to the dynamic boundary-value problem for grain conglomerates. In the numerical implementation, mesh elements are united into sets to represent different grains. The elements belonging to a certain grain have the same physical and mechanical characteristics and contiguously occupy a closed region to fit the grain shape. Neighboring grains interact with each other through a common boundary going through nodal points shared by the boundary elements. The adjacent grains are thought to be in permanent contact during the entire deformation process (i.e., cracks are supposed not to appear).

In the numerical examples presented in this paper the grain structures were constructed with the step-by-step packing method providing fast generation of 3D microstructures on a hexahedral mesh [16]. A series of calculations was performed for polycrystals containing different numbers of equiaxed grains approximated by hexahedral meshes with different resolutions. The boundary-value problem was solved by the finite-difference method using *in-house* software package DLHM-3D.

Two basic approaches involving either phenomenological [12, 13] or crystal plasticity models [17, 18] are commonly used to describe the grain constitutive behavior. In the former case, the grains are associated with a set of the stress-strain curves scattered about an average curve fitting experimental data for the polycrystalline material. In such a simplified way, the orientation dependence of grain ability to resist deformation is taken into account. Crystal plasticity models, in their turn, rely on the physical mechanisms of plastic deformation related to a crystalline structure. Along with the grain-scale inhomogeneity, the models are capable of describing an anisotropic mechanical response at the intragrain scale.

The crystal plasticity formulation is particularly important for polycrystalline materials with a limited number of slip systems (e.g., hexagonal metals) or with a pronounced

crystallographic texture. However, in the case of non-textured polycrystals with a cubic crystal lattice, the two kinds of models provide similar results, and the use of simplified models is quite feasible. In what follows, we analyze the results calculated for non-textured aluminum polycrystals in terms of the phenomenological description.

The polycrystalline grains in real materials are distinguished by their crystallographic orientations and, consequently, by their elastic and plastic properties. However, the difference between the elastic moduli of grains is frequently ignored since the elastic strain in metals is moderate compared to possible plastic strain. At the same time, this can be an important factor governing the grain-scale stress concentration and thus affecting the nucleation of plastic shear strains. In our calculations, the difference in the elastic characteristics of grains is accounted for by a random scatter of the elastic moduli about the mean within 10%.

The elastic-to-plastic transition of grains is calculated in terms of the von Mises yield criterion where the yield stress values are determined with allowance for the strain hardening and grain-boundary strengthening

$$\sigma_y^i = \sigma_0^i + k \Big/ \sqrt{D^i} + f\left(\varepsilon_{eq}^p\right), \tag{1}$$

where σ_0^i is the initial yield stress of the *i*th grain. In the numerical implementation the σ_0^i values for different grains were scattered within 20% about 10 MPa. The second term of the right-hand sum is the Hall-Petch relation, where $k = 875\ \text{MPa} \cdot \sqrt{\mu\text{m}}$ is the coefficient of grain-boundary strengthening and D^i is the *i*th grain diameter calculated as a diameter of a sphere of the same volume. The third term of the sum is the strain hardening function constructed to fit the experimental data for an Al6061-T3

$$f\left(\varepsilon_{eq}^p\right) = a\left(1 - \exp\left(-\varepsilon_{eq}^p / b\right)\right). \tag{2}$$

Here ε_{eq}^p is the equivalent plastic strain accumulated in a local region (mesh element); $a = 65$ MPa and $b = 0.048$ are the fitting constants.

In order to simulate uniaxial tension, two opposite surfaces of the model specimens were specified to undergo axial displacements. The top surface was thought to be free of external forces, and the bottom surface was a symmetry plane. The lateral sides in the calculations were set to be either free surfaces or symmetry planes.

3. Grain-Scale Stress-Strain Evolution in a Subsurface Layer

The interfaces between materials with different elastic-plastic properties are known to be the sources of stress concentrations under loading [17, 19-22]. The difference in the material characteristics, the interface curvature and the loading conditions are among the governing factors responsible for the stress values in the vicinity of interfaces. Noticeably, the difference in the elastic moduli of individual grains results in stress concentration near the grain boundaries already at the elastic stage of loading. Even a small increase in local stresses in the near-boundary regions in comparison to the average stress level favors

plastic strain nucleation here. The larger the difference in the mechanical characteristics of contacting grains, the higher the stress concentration near the boundary between them. The most favorable conditions for the nucleation of plastic strains are realized in the vicinity of triple junctions of grains markedly different in their elastic modules.

The specimen surface can be treated as an interface between materials with essentially different mechanical properties (a metal-air interface). Thus, in combination with geometrical irregularities, it can be the most powerful source of stress concentration. This agrees with the experimental and theoretical studies [5-11, 17] showing that the specimen surface plays a key role in the appearance of stress concentrations and plastic strain nucleation. This conclusion is supported by the calculation results for the polycrystalline conglomerate consisting of 280 grains (Fig. 1b). The model size is 480×375×480 μm. The equivalent stresses in local regions of the surface layer become higher than those developing in the bulk grains from the very beginning of tension. As an illustration, the stress and plastic strain patterns in the surface layer and in a section located at a depth of 250 μm below the surface are plotted in Fig. 2a and b. A scatter of local stresses and strains about their mean values is more pronounced in the surface layer than in the bulk of the material. This is the reason for first plastic deformation to nucleate on the surface as it is observed experimentally [5-8].

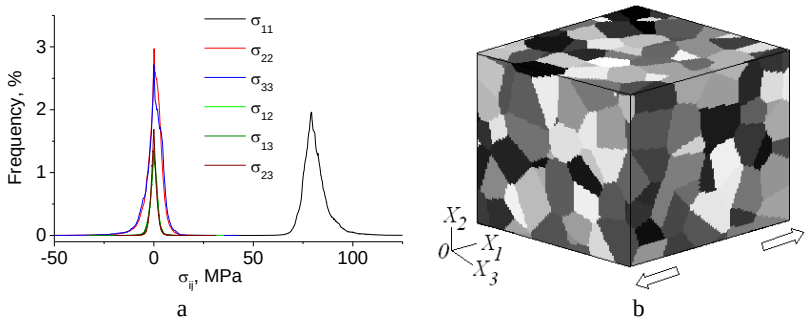

Fig. 1 Frequency distributions of the stress tensor components (a) calculated for the polycrystalline model (b) under uniaxial tension along the X_1-axis

Let us analyze the frequency distributions of different stress and strain tensor components plotted in Fig. 1a. It is not surprising that the stress and plastic strain tensor components along the tensile axis make a major contribution to the stress-strain state. The average values of other stress and strain tensor components have to be zero, which corresponds to macroscopic conditions of uniaxial tension. However, in local regions, particularly near the grain boundaries, all components of the stress and strain tensors take on nonzero values. What is more, they exhibit a symmetrical deviation of positive and negative values about the zero level. In other words, tensile regions alternate with compressive ones. The reason for the scatter of the stress and strain values about the zero mean is as follows. Macroscopically, the stress components acting perpendicular to the tensile axis must approach zero because external forces do not act on the specimen in these directions. The local tensile and compressive regions compensate each other to provide overall zero stress. Thus the macroscopic condition of mechanical equilibrium is

satisfied. The same conclusion is valid for the strain tensor components whose average value is zero. A maximum scatter of local values of the stresses and strains about the mean is observed in the subsurface layer (Fig. 2c). The scatter exhibits a nonlinear decrease as the depth below the surface increases, and levels out at a certain depth.

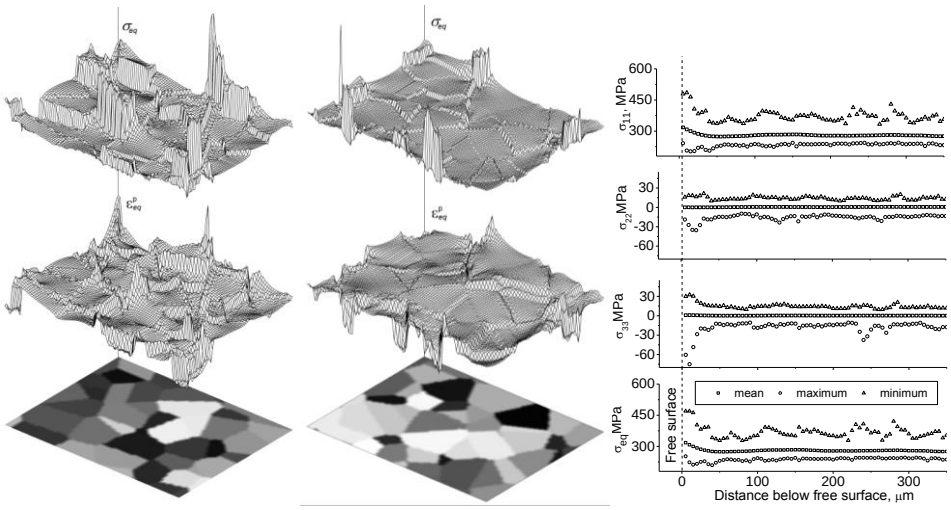

a b c

Fig. 2 Equivalent stress and equivalent plastic strain distributions in the surface layer of polycrystal (a) and at a depth of 250 μm below the surface (b) and the maximum, minimum and mean values of stress tensor components at different depth below the free surface at 2% strain

4. "STICK-SLIP" MODE OF PLASTIC DEFORMATION

A detailed study of plastic strain nucleation near grain boundaries is conducted for the model containing 10 grains approximated by a regular 100×100×100 mesh with a step of 1 μm (Fig. 3a). The mechanical properties of grains in Fig. 3 correspond to the color scale as follows: the darker the grain, the lower the elastic moduli and the yield stresses. In macroscopic terms, the model under consideration is not representative but it allows investigating the nucleation and development of plastic shear strains at the stage of microplastic deformation with reasonable time and space resolutions.

The nucleation and propagation of microplastic strains are described with allowance for a "stick-slip" mode of plastic deformation, basing on the experimental observations for dislocation behavior. It has been shown in [23] that dislocations initially presenting in some steels and aluminum alloys are immobile. The stress necessary to start off the movement of existing dislocations or to nucleate new defects is assumed to be higher than the stress required to keeping propagation of the dislocations already involved in motion. A similar "stick-slip" mode of plastic deformation is typical for, e.g., Lüders band propagation [24-26] or PLC effect [23] where an extra stress is necessary to detach dislocations from interstitial atoms. An analogy can be drawn with friction [1], where the

static friction force must be overcome by certain applied forces to disrupt the surface bonds between contacting bodies, whereupon their subsequent relative motion may occur at a lower force. In the numerical implementation, such a "stick-slip" dislocation behavior was simulated through a two-limit yield criterion [26], according to which two critical values are introduced in the von Mises yield criterion. The higher stress limit, σ_H, is specified for an elastically deformed material and the lower value, σ_L, for a material involved in plastic deformation. Mathematically, σ_0 in Eq. (1) is set equal to σ_H for the regions where $\varepsilon_{eq}^p = 0$ and $\sigma_0 = \sigma_L$ if $\varepsilon_{eq}^p > 0$. As soon as a local region of the material becomes plastic, the yield stress drops down to the lower limit value and subsequent plastic deformation proceeds at the lower stress.

At the elastic loading stage, the grains exhibit nonuniform stress distributions due to the difference in the elastic moduli of contacting grains. The maximum stress develops near the triple junctions of grains with greatly different elastic properties (Fig. 3c). These regions are sources of plastic strain nucleation in the bulk of the polycrystalline material. One more stress concentration source and hence a plastic strain source is larger-scale geometric features — corner points and edges of the polycrystalline model.

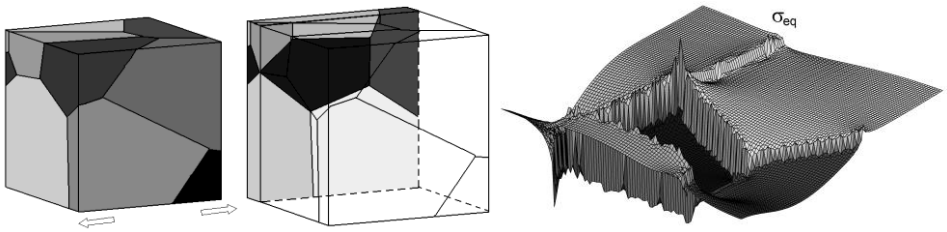

Fig. 3 Polycrystalline model (a) and stress concentration in the vicinity of triple junction of grains (c) in the internal section (b)

Figure 4 illustrates the evolution of plastic flow in a bulk section and on the surface of the polycrystalline aggregate. First, plastic strains appear in isolated regions mainly near the parts of grain boundaries where higher stresses take place. The plastic strains at this loading stage have but a little effect on the deviation of the macroscopic stress-strain curve from the linear behavior, and thus this deformation stage can be classified as microplastic. On further loading, plastic strains in the form of localized shear bands begin to propagate from the near-boundary sources into the bulk of grains. Simultaneously, new grain boundary regions become involved in plastic deformation. The analysis of shear band propagation with a high time resolution reveals a vortex motion in the elastic material ahead of the plastic front, which is well seen in the velocity field in Fig. 4b at a strain of 0.35%. This motion is necessary to accommodate the elastoplastic deformation of the neighboring regions. The existence of the vortex patterns has been predicted by molecular dynamics simulations in [27, 28] and got experimental support in [5, 6]. At this deformation stage, the stress concentration and plastic strain patterns are still affected by

the grain geometry, whereas the stress-strain curve approaches the macroscopic yield point.

Finally, some of the plastic fronts propagating from the grain boundaries form a through-the-thickness network on a larger scale. Subsequent plastic deformation mainly localizes in these regions, resulting in crystal separation into several parts shifting to each other on further loading. New regions of plastic strain nucleation are unlikely to appear at this deformation stage and the finer bands stop developing either. Correspondingly, the microplastic deformation stage gives way to the macroplasticity where the stress-strain curve goes over to the horizontal portion.

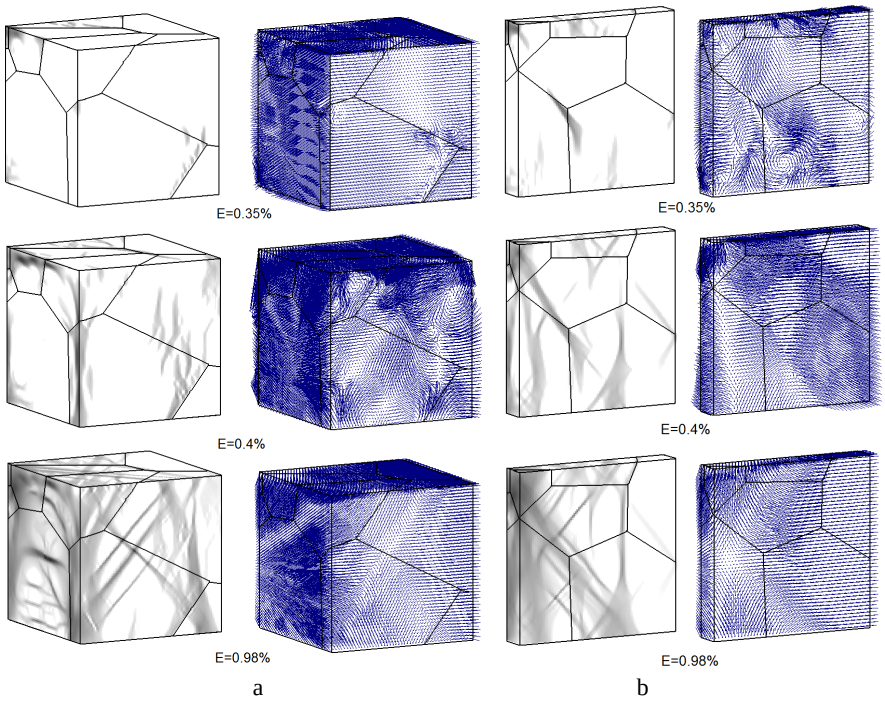

Fig. 4 Plastic strain patterns and velocity vector fields on the surface (a) and in an internal section (b) of a polycrystal at the microplastic deformation stage

5. Mesoscale Deformation-Induced Surface Roughening

The phenomenon of deformation-induced surface roughening acquires a special significance in tribological applications. Being one of the essential factors influencing friction and adhesion (see, e.g., [1, 2, 29, 30]), this phenomenon can be treated as a positive or negative effect depending on the requirements on operative conditions. Along with other methods to control adhesion and friction behavior (see, e.g., [30, 31]), the idea of controllable roughening sounds attractive which requires a deep understanding of the roughening mechanisms at different scales.

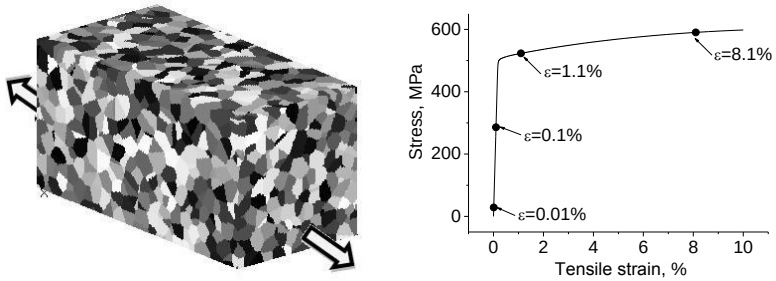

a b

Fig. 5 Polycrystalline model (a) and its stress-strain curve (b)

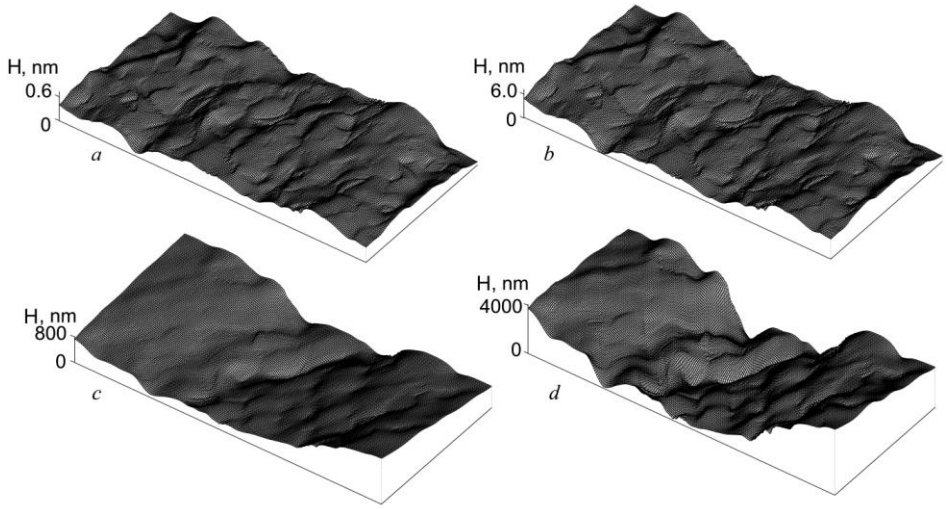

Fig. 6 Surface roughness in the polycrystalline model at a tensile strain of 0.01(a), 0.1(b), 1.1(c), and 8.1% (d)

The deformation-induced roughening is especially pronounced in polycrystalline metals where the surface out-of-plane displacements develop throughout all length scales from micro to macro [8-11]. A special role belongs to the mesoscale roughening, where the surface undulations occasionally take a form of ridges, ropes, wrinkles, checkered distributions of hills and hollows, etc. The width of the surface folds for different materials is reported to vary from several tens to several hundreds of micrometers while the height evolves from a few to several tens of microns in the course of deformation. Of fundamental importance is the fact that not individual grains but their conglomerates are involved in cooperative motion to form the surface folds. Thus, the mechanisms of the mesoscale surface roughening can hardly be described either in terms of dislocation theory or within macroscopic continuum mechanics alone. In this contribution, the evolution of mesoscale surface morphology is examined numerically in terms of mesomechanics.

Mesomechanics [32] treats inhomogeneous materials with interfaces of different nature and configurations. The presence of a microstructure gives rise to specific non-homogeneous deformation modes at larger scales. We suggest that the term "mesoscale" does not imply a certain length-scale of investigation in contrast to, e.g., terms of "micromechanics" or "nanomechanics", but relates to the specific phenomena produced by collective low-scale structural effects. For example, the mesomechanical approach is successfully applied in geodynamical problems [33], where representative structure elements are enormous tectonic plates. Contrastingly, a nanomaterial where a characteristic length scale is about several nanometers can be considered within the mesomechanical approach as well [34]. In polycrystalline metals, the mesoscale phenomena are attributed to the cooperative effects of grain conglomerates.

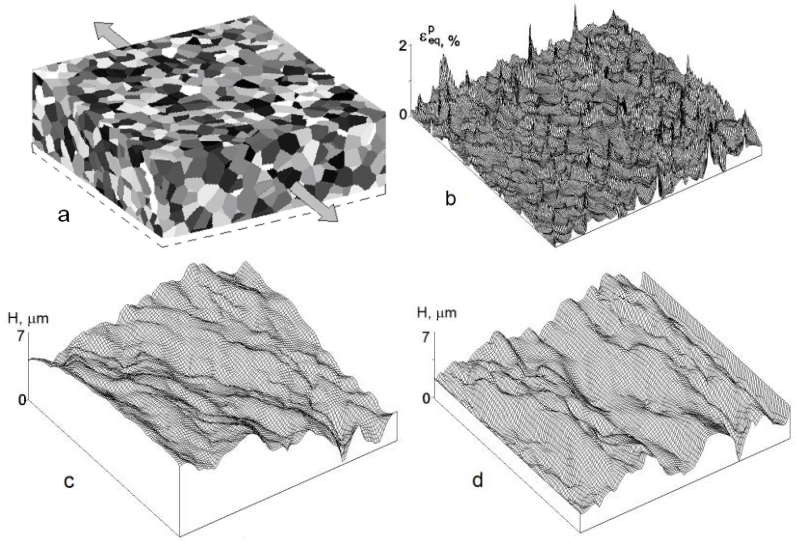

Fig. 7 Equivalent plastic strain (b) and roughness patterns (c, d) on the free surface of the polycrystalline specimen (a) at a tensile strain of 0.4%; the boundary conditions at the lateral sides simulate the symmetry planes (b, d) or free surface (c)

Figure 6 illustrates roughness formation at the initial stage of tension on the top free surface of the polycrystalline model measuring 1000×500×500 μm presented in Fig. 5a. Corresponding deformation states are depicted on the stress-strain curve in Fig. 5b. The material free surface is getting rough already at the elastic deformation stage (Fig. 6a), although these kinds of surface undulations are difficult to be identified experimentally. One can reveal two distinct roughening patterns – the finer is attributed to the relative shift of individual grains, and the larger scale folds can be classified as mesoscale roughness. In the latter case, groups of grains located close to the specimen surface are set in the cooperative motion perpendicular to the free surface to form extended ridges and valleys. The mesoscale folds going through the entire surface of the specimen at a certain angle to the tensile axis exhibit a spatial periodicity. The transverse size of the mesoscale

surface ridges and valleys exceeds the average grain size by severalfold, which agrees with experiments.

Obviously, the microstructure plays a primary role in the formation of the mesoscale roughening with the subsurface layer of grains making a major contribution to this process. The grain influence on the roughness pattern diminishes nonlinearly with the depth below the free surface. Calculations where the thickness of the computational domain was varied revealed that grains lying within two average grain diameters below the free surface were a major contributor to the formation of mesoscale surface folds. For a larger thickness of the polycrystalline models, the deformation relief formed on the free surface remained nearly unchanged.

One more factor which may affect the free surface pattern is the method of load application. In two sets of calculations for the polycrystalline model of 1500×500×1500 μm shown in Fig. 7a the lateral surfaces were set to be symmetry planes (Fig. 7d) or free of a load (Fig. 7c). In the former case, the top free surface shows a tendency to form longitudinal folds perpendicular to the load direction (Fig. 7d), whereas in the latter the surface folds are formed at an angle of 45 degrees to the axis of tension (Fig. 7c).

6. CONCLUSION

The mesoscale deformation-induced surface phenomena have been numerically analyzed on the examples of three-dimensional polycrystals under uniaxial tension. The equiaxial grain structures typical for aluminum alloys were implemented in the calculations. The three-dimensional formulation of the boundary-value problem enabled direct simulating the free surface effects in the polycrystals under deformation.

In accordance with experimental evidence, the calculation results showed plastic strain nucleation primarily near the grain boundaries which were the sources of stress concentrations at the grain scale. The highest stress level is observed near the triple junctions of grains with strongly different mechanical characteristics. The stress and strain tensor components acting along the axis of tension made a major contribution to the deformation response both at the micro- and macroscales. While the rest stress and strain components were zero at the macroscale, they demonstrated positive and negative values deviating about the zero level at the grain scale with the highest quantities taking place near grain boundaries. The local tensile and compressive regions compensated each other to satisfy the macroscopic condition of mechanical equilibrium.

The specimen surface was found to be the most powerful source of stress concentrations and thus played a key role in the nucleation of plastic strains. A scatter of local stresses and strains about their mean values was considerably more pronounced in the subsurface layer than at a distance below the free surface. This was the reason for plastic deformation to originate on the specimen surface which is consistent with experimental observations.

Finally, the appearance of mesoscale surface roughening at the initial stage of plastic deformation was analyzed. It was shown that originally flat free surface began to experience mesoscale morphological changes at the outset of the loading process. The calculation results suggested that the polycrystalline microstructure in the subsurface layer was responsible for the formation of the mesoscale surface folds. The width of the

resulting folds exceeded the characteristic size of polycrystalline grains and interfacial asperities. The height of the surface folds increased in the course of deformation, but the qualitative pattern remained unchanged until one deformation mechanism gave way to another when the elastic–plastic transition took place.

Acknowledgement: *The work was performed by the Government research assignment for ISPMS SB RAS (№FWRW-2021-/0002/).*

REFERENCES

1. Popov, V., 2010, *Contact mechanics and friction*. Springer, Berlin, Heidelberg, p. 362.
2. Popov, V., Pohrt, R., Li, Q., 2017, *Strength of adhesive contacts: Influence of contact geometry and material gradients*, Friction 5, pp. 308–325.
3. Joe, J., Thouless, M.D., Barber, J.R., 2020, *Effect of surface roughness on adhesive instabilities for the elastic layer*, Front. Mech. Eng., 6, 31.
4. Ostermeyer, G.-P., Popov, V.L., Shilko, E., Vasiljeva, O. (Eds.), 2021, *Multiscale Biomechanics and Tribology of Inorganic and Organic Systems*, Springer International Publishing, p. 565.
5. Shanyavskiy, A.A., Soldatenkov, A.P., 2020, *Scales of metal fatigue limit*, Phys Mesomech, 23, pp. 120–127.
6. Shanyavsky, A.A., 2015, *Scales of metal fatigue cracking*, Phys Mesomech, 18, pp. 163–173.
7. Sauzay,M., Gilormini P., 2001, *Surface and cyclic microplasticity*, Fatigue Fract. Eng. Mater. Struct., 23, pp. 573-579.
8. Chen, J.Q., Gao, H.T., Hu, X.L., Yang, L.Q., Ke, D.W., Liu, X.H., Yan, S., Lu, R.H., Misra, R.D.K., 2020, *The significant size effect on nucleation and propagation of crack during tensile deformation of copper foil: Free surface roughening and crystallography study*, Mater. Sci. Eng. A, 790, 139678.
9. Stoudt, M.R., Levine, L.E., Creuziger, A., Hubbard, J.B., 2011, *The fundamental relationships between grain orientation, deformation-induced surface roughness and strain localization in an aluminum alloy*, Mater. Sci. Eng. A, 530, pp. 107-116.
10. Solhjoo, S., Halbertsma, P. J., Veldhuis, M., Toljaga, R., Pei, Y., 2020, *Effects of loading conditions on free surface roughening of AISI 420 martensitic stainless steel*, Mater. Proc. Tech., 275, 116311.
11. Yoshida, K., 2014, *Effects of grain-scale heterogeneity on surface roughness and sheet metal necking*, Int. J. Mech. Sci., 83, pp. 48-56.
12. Panin, A.V., Romanova, V.A., Balokhonov, R.R., Perevalova, O.B., Sinyakova, E.A., Emelyanova, O.S., Leontieva-Smirnova, M.V., Karpenko, N.I., 2012, *Mesoscopic surface folding in EK-181 steel polycrystals under uniaxial tension*, Phys Mesomech, 15, pp. 94–103.
13. Romanova, V.A., Balokhonov, R.R., Batukhtina, E.E., Emelianova E.S., Sergeev M.V., 2019, *On the Solution of Quasi-Static Micro- and Mesomechanical Problems in a Dynamic Formulation*, Phys Mesomech, 22, pp. 296–306.
14. Romanova, V., Balokhonov, R., Emelianova, E., Zinovieva, O., Zinoviev, A., 2019, *Microstructure-based simulations of quasistatic deformation using an explicit dynamic approach*, Facta Univesitatis-Series Mechanical Engineering, 17(2), pp. 243-254.
15. Radchenko, P.A., Batuev, S.P., Radchenko, A.V., 2021, *Numerical analysis of concrete fracture under shock wave loading*, Phys. Mesomech. 24(1), doi: 10.1134/S1029959921010069.
16. Romanova, V., Balokhonov, R., 2021, *A method of step-by-step packing and its application in generating 3D microstructures of polycrystalline and composite materials*, Engineering with Computers, 37, pp. 241–250.
17. Guilhem, Y., Basseville, S., Curtit, F., Stéphan, J-M., Cailletaud, G., 2013, *Numerical investigations of the free surface effect in three-dimensional polycrystalline aggregates*, Comput. Mater. Sci., 70, pp. 150-162.
18. Trusov, P.V., Sharifullina, E.R., Shveykin, A.I., 2019, *Multilevel Model for the Description of Plastic and Superplastic Deformation of Polycrystalline Materials*, Phys Mesomech, 22, pp. 402–419.
19. Shavshukov, V.E., 2020, *Extreme Strain Fluctuations in Polycrystalline Materials*, Phys Mesomech, 23, pp. 13–20.

20. Barbe, F., Decker, L., Jeulin, D., Cailletaud, G., 2001, *Intergranular and intragranular behavior of polycrystalline aggregates. Part I: FE model*, Int. J. of Plasticity, 17(4), pp. 513–536.
21. Guo, Y., Collins, D.M., Tarleton, E., Hofmann, F., Tischler, J., Liu, W., Xu, R., Wilkinson, A.J., Britton, T.B., 2015, *Measurements of stress fields near a grain boundary: Exploring blocked arrays of dislocations in 3D*, Acta Mater., 96, pp. 229-236.
22. Zavdoveev, A., Rogante, M., Poznyakov, V., Heaton, M., Acquier, P., Kim, H. S., Baudin, T., Kostin, V., 2020, *Development of the PC-GMAW welding technology for TMCP steel in accordance with welding thermal cycle, welding technique, structure, and properties of welded joints*, Reports in Mechanical Engineering, 1(1), pp. 26-33.
23. D. Caillard, J.L. Martin (Eds), 2003, *Thermally Activated Mechanisms in Crystal Plasticity*, Pergamon Materials Series 8, Pergamon.
24. Brlić, T., Rešković, S., Jurković, S., Janeš, G., 2020, *Mathematical modeling of the influence parameters during formation and propagation of the Lüders bands*, Facta Universitatis-Series Mechanical Engineering, 18(4), pp. 595-610.
25. Farber, V.M., Morozova, A.N., Khotinov, V.A. et al., 2020, *Plastic Flow in a Chernov–Luders Band in Ultrafine-Grained 08G2B Steel*, Phys Mesomech, 23, pp. 340–346.
26. Romanova, V., Balokhonov, R., Schmauder, S., 2011, *Three-dimensional analysis of mesoscale deformation phenomena in welded low-carbon steel*, Mater. Sci. Eng. A, 528, pp. 5271-527.
27. Dmitriev, A.I., Nikonov, A.Y., Shugurov, A.R. *et al.*, 2019, *The Role of Grain Boundaries in Rotational Deformation in Polycrystalline Titanium under Scratch Testing*, Phys Mesomech, 22, pp. 365–374.
28. Dmitriev, A.I., Nikonov, A.Y., Filippov, A.E. *et al.*, 2019, *Molecular dynamics study of the evolution of rotational atomic displacements in a crystal subjected to shear deformation*, Phys Mesomech, 22, pp. 375–381.
29. Popov, V.L., 2020, *Coefficients of restitution in normal adhesive impact between smooth and rough elastic bodies*, Reports in Mechanical Engineering, 1(1), pp. 103-109.
30. Popov, M., Li, Q., 2018, *Multimode active control of friction, dynamic ratchets and actuators*, Phys. Mesomech. 21, pp. 24–31.
31. Cinat, P., Gnecco, G., Paggi, M., 2020, *Multi-Scale Surface Roughness Optimization Through Genetic Algorithms*, Front. Mech. Eng., 6, 29.
32. Haritos, G.K., Hager, J.W., Amos, A.K., Salkind, M.J., Wang, A.S.D., 1988, *Mesomechanics: the microstructure-mechanics connection*, Int. J. Solids Structures, 24, pp. 1081-1096.
33. Bykov, V.G., 2020, *Development of sliding regimes in faults and slow strain waves*, Phys. Mesomech., 23(3), pp. 271–278.
34. Panin, V.E., Shulepov, I.A., Derevyagina, L.S., S. V. Panin, A. I. Gordienko, I. V. Vlasov, 2020, *Nanoscale Mesoscopic Structural States in Low-Alloy Steels for Martensitic Phase Formation and Low-Temperature Toughness Enhancement*, Phys Mesomech, 23, pp. 376–383.